(43) Matheson, M. S.; Auer, E. E.; Bevilacqua, E. B.; Hart, E. J. J. Am. Chem. Soc. 1949, 71, 497.
(44) Fukuda, T.; Ma, Y.-D.; Nagata, M.; Inagaki, H. Polym. J. 1982, 9, 729.
(45) To avoid confusion, some of the notations given in the original paper[44] have been slightly modified.
(46) North, A. M.; Reed, G. A. Trans. Faraday Soc. 1961, 57, 859.
(47) Ludwico, W. A.; Rosen, S. L. J. Polym. Sci., Polym. Chem. Ed. 1976, 14, 2121.
(48) Flory, P. J. "Principles of Polymer Chemistry"; Cornell University Press: Ithaca, NY, 1953.
(49) Leich, R.; Fuhrmann, J. J. Polym. Sci., Polym. Chem. Ed. 1983, 21, 2215.
(50) Korus, R.; O'Driscoll, K. F. In "Polymer Handbook"; Brandrup, J., Immergut, E. H., Eds.; Academic Press: New York, 1975; Chapter II.
(51) To compute eq 19, we assumed that p_i is given by the terminal-model eq 16. This is not correct in a strict sense, since the failure of the model has been established. However, it should be a valid approximation, since p_i should not be very sensitive to models.
(52) Fukui, K.; Yonezawa, T.; Morokuma, M. J. Polym. Sci. 1961, 49, S11.
(53) North, A. M. In "Reactivity and Structure in Polymer Chemistry"; Jenkins, A. D., Ledwith, A., Eds.; Wiley: London, 1974; Chapter 5.
(54) Horie, K.; Mita, I. Kobunshi 1978, 27, 637.
(55) O'Driscoll, K. F. Pure Appl. Chem. 1981, 53, 617.
(56) Berlin, A. A.; Volfson, S. A.; Enikolopian, N. S. Adv. Polym. Sci. 1981, 38, 89.
(57) Seiner, J. A.; Litt, M. Macromolecules 1971, 4, 308.
(58) Tüdös, F.; Kelen, T.; Berezhnikh, T. F. J. Polym. Sci., Polym. Symp. 1975, 50, 109.
(59) Kamachi, M. Adv. Polym. Sci. 1981, 38, 56.

Free-Radical Copolymerization. 4. Rate Constants of Propagation and Termination for the *p*-Chlorostyrene/Methyl Acrylate System

Yung-Dae Ma, Takeshi Fukuda,* and Hiroshi Inagaki

Institute for Chemical Research, Kyoto University, Uji, Kyoto 611, Japan.
Received April 23, 1984

ABSTRACT: The propagation and termination mechanisms of the free-radical copolymerization of *p*-chlorostyrene and methyl acrylate in the bulk at 40 °C were examined by studying the steady-state as well as non-steady-state polymerizations and thus evaluating the rate constants of propagation and termination individually as a function of feed-monomer composition. The observed rate constant of propagation as well as the copolymer composition studied previously indicated the failure of the terminal model to describe the propagation step of this system. As far as numerical values are concerned, this system is well described by the penultimate model. If one analyzes the data on the steady-state polymerization rate according to the Walling equation, one obtains "apparent" values of the cross-termination factor ϕ ranging from about 70 to as large as 500. The values of the termination rate constant actually observed are well described by the chemically controlled termination model with $\phi = 1$ as well as by the North diffusion model. These results confirm the main conclusions obtained in the previous study on the styrene/methyl methacrylate system.[1]

Introduction

In the preceding paper,[1] the kinetics of free-radical copolymerization of styrene and methyl methacrylate was examined by studying the steady-state as well as non-steady-state polymerizations and thus evaluating the rate constants of propagation and termination individually as a function of monomer composition. This unusual but comprehensive approach has disclosed the striking fact that the so-called terminal model[2,3] is incapable of describing the propagation step of this system, and that the termination step is, as opposed to previous results, well characterized by the Walling factor[4] ϕ close to 1. These results throw a strong doubt on the essential validity of the terminal-model propagation scheme and the prevailing arguments based on it about the mechanism of the termination step. It now seems important to examine a variety of copolymerization systems, especially those exhibiting large values of ϕ according to the conventional analysis, by collecting precise experimental data on the individual rate constants.

In this paper, we examine the bulk copolymerization of *p*-chlorostyrene (pCS, monomer 1) and methyl acrylate (MA, monomer 2) at 40 °C by the same approach as for the above system. The pCS/MA system is interesting because, as has already been reported,[5] its composition curve exhibits small but distinct deviations from the terminal-model curve (the Mayo–Lewis curve[3]). A more definite answer about the model propriety is expected in this study, since the rate equation should generally be more model sensitive than the composition equation is. Another point of interest with this system is that the ϕ value estimated by the conventional method, in which the validity of the terminal model is assumed,[4] is exceptionally large and composition dependent. According to our preliminary results,[6] it is even larger than 500 for a certain range of monomer composition. Whether this is a real phenomenon or not can be ascertained only through the direct evaluation of the termination rate constant.

Experimental Section

Materials. The pCS monomer was synthesized from *p*-dichlorobenzene and purified by a standard process.[5] The commercially obtained MA monomer was purified with special care.[5] 2,2′-Azobis(isobutyronitrile) (AIBN) and 2,2′-azobis(cyclohexane-1-carbonitrile) (ACN) purchased from Nakarai Chemicals Co., Japan, and 4-hydroxy-2,2,6,6-tetramethylpiperidinyl-1-oxy (HTMPO) from Eastman Kodak Co., Rochester, NY, were purified by recrystallization as described previously.[1]

Steady-State Polymerization. The rate of the steady-state polymerization initiated by AIBN was determined by the ampule method. The composition of the copolymer was determined by combustion analysis for carbon and potentiometric titration with silver nitrate for chlorine. The number-average molecular weight M_n and the polydispersity index M_w/M_n were estimated by gel permeation chromatography (GPC) with a column system calibrated with standard polystyrenes. The initiation rate was de-

0024-9297/85/2218-0026$01.50/0

Table I
Summary of the Batch Copolymerization of pCS and MA in the Bulk at 40 °C

run	f_1[a]	[M],[b] mol/L	10^2[I],[c] mol/L	t,[d] min	Y,[e] wt %	F_1[f]	$10^4R_p/[I],^{1/2}$ $(mol/L)^{1/2}/s$	$10^{-5}M_n$[g]	M_w/M_n[g]
1	0	10.823	1.415				122.7[h,i]		
2			1.415						
3			0.859						
4			0.338						
5	0.024	10.721	0.498	30	0.43	(0.131)	3.428		
6	0.050	10.611	0.544	80	0.82	(0.217)	2.229		
7	0.073	10.511	2.959	54	1.35	0.283	2.211	4.16	1.95
8	0.085	10.460	2.905	25	0.54	0.277	2.003		
9	0.100	10.403	0.865	140	1.39	(0.331)	1.798[h]		
10			1.540	110	1.47	(0.350)			
11			2.298	80	1.42	(0.336)		3.94	2.02
12			3.337	90	1.86	(0.341)			
13			4.324	50	1.23	(0.323)		2.63	1.74
14	0.137	10.254	1.293	110	1.36	(0.404)	1.616		
15	0.179	10.089	3.982	120	2.42	0.429	1.491		
16	0.184	10.069	3.112	120	2.26	0.442	1.488[h]		
17			3.412	59	1.04	0.445		2.99	1.98
18	0.239	9.870	4.160	120	2.36	0.471	1.413		
19	0.272	9.746	3.721	59	1.08	0.511	1.371	2.86	1.86
20	0.301	9.643	4.359	59	1.18	0.563	1.354	2.84	1.73
21	0.414	9.263	3.808	60	1.13	0.616	1.353		
22	0.443	9.169	4.440	120	2.43	0.638	1.344		
23	0.462	9.112	4.932	60	1.32	0.632	1.394		
24	0.532	8.900	4.247	60	1.20	0.679	1.351	3.10	1.69
25	0.638	8.592	4.296	60	1.19	0.746	1.309		
26	0.709	8.401	4.702	60	1.32	(0.806)	1.358		
27	0.714	8.385	4.052	120	2.27	0.766	1.286		
28	0.757	8.267	3.005	50	0.87	0.807	1.350		
29	0.858	8.015	4.308	59	1.23	(0.838)	1.355		
30	0.861	8.006	3.666	60	1.16	0.866	1.343	2.60	1.87
31	0.868	7.991	3.254	60	1.08	0.855	1.329		
32	1	7.683	2.098	130	1.85		1.315[h]		
33			2.981	100	1.76				
34			3.731	80	1.60			2.49	1.67
35			4.436	120	2.60	1.004			

[a] Mole fraction of pCS in feed. [b] Total monomer concentration. [c] AIBN concentration. [d] Reaction time. [e] Conversion. [f] Mole fraction of pCS in copolymer determined by the chlorine analysis (the value in parentheses was determined by the carbon analysis, which is less reliable than the chlorine analysis for this particular system[5]). [g] GPC value. [h] Average value. [i] By dilatometry.

termined by using HTMPO as an inhibitor. Details of all these experiments were described elsewhere.[1,5]

Volume Contraction Factor. The volume contraction factor was evaluated on the basis of the previously proposed equation.[1,7,8] The values of the parameters included in the equation were determined by measuring the densities of appropriate solutions and reported elsewhere.[8]

Non-Steady-State Polymerization. The radical lifetime was determined by the rotating-sector method. ACN was used as a photosensitive initiator. The apparatus employed and experimental details were as described previously.[1] We previously reported that the steady-state polymerization rate R_p of the styrene/methyl methacrylate system depends significantly on the conversion C even in a low-C region.[1] The present system showed qualitatively the same dependence in all cases, which was corrected for according to the method quoted as "method 1" in ref 1.

Results and Discussion

As described in some detail in the preceding paper,[1] it is convenient to define the rate constants of propagation, k_p, and termination, k_t, for copolymerization by the same equations as for homopolymerization

$$R_p = -d[M]/dt = k_p[P\cdot][M] \quad (1)$$

$$R_t = k_t[P\cdot]^2 \quad (2)$$

where R_p is the propagation rate, which is assumed to be equal to the polymerization rate, R_t is the termination rate, and [P·] and [M] are the total concentrations of (polymeric) radicals and monomers, respectively. In the *stationary state* in which the relative populations of individual types of radicals are constant,[1] k_p and k_t are constant for a given composition of the feed. In the *steady state* in which the total concentration [P·] as well as the relative populations of the radicals is constant, we may equate R_t to the rate of initiation R_i to yield from eq 1 and 2 the familiar relation

$$R_p = \omega R_i^{1/2}[M] \quad (3)$$

with

$$\omega = k_p/k_t^{1/2} \quad (4)$$

$$R_i = 2f'k_d[I] \quad (5)$$

where [I] is the concentration of the initiator whose rate constant of decomposition is k_d, and efficiency, f'. Insofar as k_p and k_t are constant, the radical lifetime τ can be determined by the same method as for homopolymerization, and the rate constant ratio k_p/k_t is evaluated according to the familiar relation

$$\tau R_p = (k_p/k_t)[M] \quad (6)$$

Thus, as in the case of homopolymerization, k_p and k_t can be individually evaluated by the combination of the steady- and non-steady-state experiments. The functional forms of k_p and k_t depend on the details of the propagation and termination mechanisms. Explicit expressions for k_p and k_t for some familiar kinetic models were given in ref 1.

We now turn to our experiments. All steady- and non-steady-state copolymerization runs were carried out at conversions low enough (<2.5% by weight) so that composition drifts with conversion may be neglected. Table

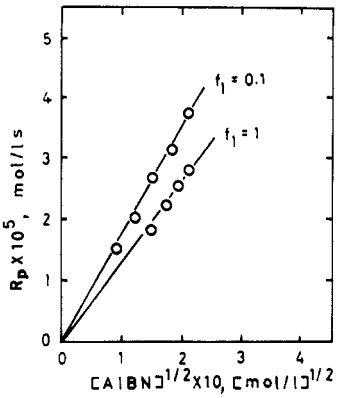

Figure 1. Plot of R_p vs. $[AIBN]^{1/2}$ for pCS/MA/AIBN/40 °C systems.

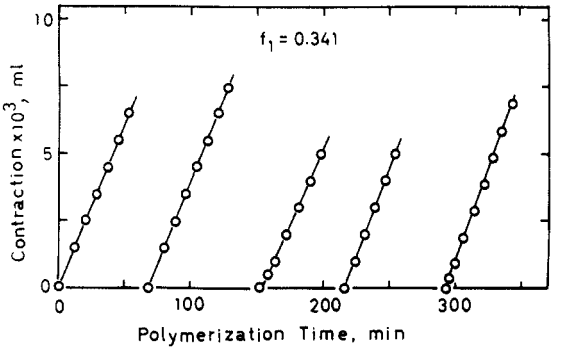

Figure 2. Plot of volume contraction vs. polymerization time for pCS/MA/AIBN/HTMPO/40 °C systems with $f_1 = 0.341$ and $10^2 \times$ [HTMPO]/[AIBN] = 0, 0.312, 0.585, 0.778, and 1.150 (from left to right).

I summarizes the results of the steady-state runs initiated by AIBN. The values of M_n estimated by the GPC analysis are of the order of 10^5 in all cases, a figure large enough for the long-chain approximations[1,3] to be applicable. The values of M_w/M_n ratio are between 1.5 and 2.0 for all the samples examined. The M_n values of the polymers recovered after a series of rotating-sector runs were found to be large enough, too, while their M_w/M_n ratios were, as expected, considerably larger than those of the steady-run samples of comparable composition (cf. Table III).

The composition curve of this system was examined previously.[5] To summarize the results, values of $r_1 = 1.21$ and $r_2 = 0.144$ were obtained as an optimum set of terminal-model parameters (reactivity ratios). However, deviations exceeding the limit of experimental error existed between the observed and calculated compositions, which could be explained, at least numerically, by the penultimate model with $r_1 = 0.92$, $r_1' = 2.3$, and $r_2 (=r_2') = 0.18$. The question as to whether r_2 is in fact equal to r_2' remained unanswered because of lack of experimental accuracy.[5] In what follows, we will employ these two sets of parameter values to test the validity of the individual models. The compositions of the sector-run samples were found to be consistent with those of the steady-run samples (cf. Tables I and III).

In Figure 1, the rate of steady-state polymerization R_p is plotted against the square root of the initiator concentration $[AIBN]^{1/2}$ for two different values of f_1, showing that proportionality holds between these quantities, within experimental error.

The initiation rate constant $2f'k_d$ was determined by the inhibitor method. Results are summarized in Table II. Each inhibition time was determined by dilatometrically following the onset of polymerization. Some examples of the contraction vs. time curve are given in Figure 2. For

Table II
Inhibition Times of the pCS/MA/AIBN/HTMPO System (40 °C)

f_1[a]	10^2[AIBN], mol/L	10^4[HTMPO], mol/L	t_i,[b] min	$10^6(2f'k_d)$,[c] s^{-1}
0	0.986	0.164	46	0.619
	1.355	0.415	81	
	1.597	0.576	95	
	0.952	0.455	130	
	1.567	0.804	139	
0.162	2.318	0.308	30	0.640
	2.208	0.446	51	
	2.229	0.637	78	
	2.174	0.790	91	
0.341	2.152	0.672	69	0.637
	2.091	1.224	154	
	2.131	1.658	216	
	2.062	2.371	292	
0.555	2.524	0.713	62	0.747
	2.358	1.267	122	
	2.251	1.950	197	
	2.327	2.602	247	
0.674	2.253	0.570	58	0.668
	2.285	1.044	125	
	2.105	1.797	204	
	2.448	2.699	275	
0.693	2.601	0.588	55	0.743
	2.546	0.847	70	
1	2.260	0.299	27	0.767
	2.318	0.479	44	
	2.418	0.621	56	

[a] Mole fraction of pCS. [b] Inhibition time. [c] Average value.

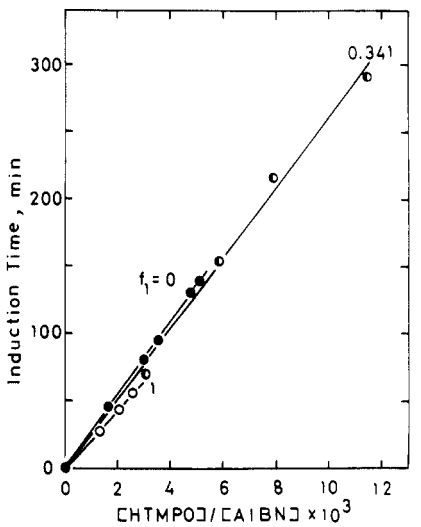

Figure 3. Plot of induction time vs. inhibitor-to-initiator concentration ratio for pCS/MA/AIBN/HTMPO/40 °C systems.

all compositions including $f_1 = 0$ and 1, the curves were linear after the onset of polymerization to give well-defined inhibition times. In Figure 3, the inhibition time t_i is plotted against the inhibitor-to-initiator concentration ratio, [HTMPO]/[AIBN], for some values of f_1. In all these and other cases examined, proportionality was found to hold between these quantities. The values of $2f'k_d$ determined from the slopes of the plot are collected in Figure 4, which indicates that the present system is well represented by the linear function

$$2f'k_d = 0.148f_1 + 0.619 \qquad (\times 10^{-6}\ s^{-1})$$

From the value of $R_p/[I]^{1/2}$ given in Table I along with the above relation, the parameter ω was evaluated, which is plotted as a function of f_1 in Figure 5. The solid curve in the figure is the best-fit representation of the experimental data (open circles), while the broken curves rep-

Table III
Summary of the Lifetime Measurements for the Copolymerization of pCS and MA at 40 °C and the Characteristics of the Recovered Polymers

					polymer characteristics		
f_1[a]	10^3[ACN], mol/L	$10^5\langle R_{pL}\rangle$, (mol/L)/s	$R_{pD}/\langle R_{pL}\rangle$	τ_L, s	F_1[b]	$10^{-5}M_n$[c]	M_w/M_n
0.046	8.513	4.047	0.125	1.61	0.218	6.21	2.39
0.114	7.695	3.066	0.147	1.32	0.351	5.58	2.52
0.233	8.274	2.483	0.134	1.35	0.501	4.63	2.15
0.360	9.101	2.416	0.156	1.62	0.601	4.63	2.16
0.443	7.948	2.350	0.151	1.49	0.657	4.96	2.37
0.593	6.549	2.142	0.129	1.27		5.13	2.33
0.757	7.662	2.104	0.125	1.31		4.55	2.19
1	8.409	1.785	0.130	1.31			
	8.738	1.937	0.129	1.31		4.42	2.20

[a] Mole fraction of pCS in feed. [b] Mole fraction of pCS in copolymer determined by the carbon analysis. [c] GPC value.

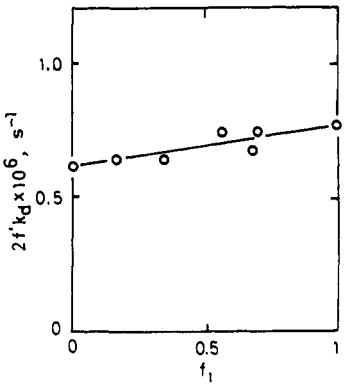

Figure 4. Plot of $2f'k_d$ vs. f_1 for the pCS/MA/AIBN/40 °C system.

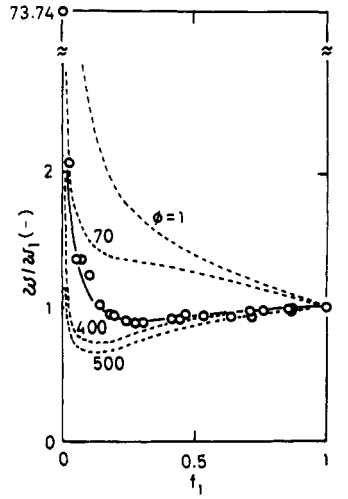

Figure 5. Plot of ω/ω_1 vs. f_1 for the pCS/MA/40 °C system. The solid curve is the best-fit representation of the experimental data (open circles), while the broken curves represent the Walling equation[1] with the values of ϕ indicated in the figure. $\omega = k_p/k_t^{1/2}$ and $\omega_1 = 1.95 \times 10^{-2}$ L$^{1/2}$ mol$^{-1/2}$ s$^{-1/2}$.

resent the Walling equation[1,4] for various values of ϕ. The figure shows that the values of ϕ for this system range from about 70 to about 500. Of course, this estimation is valid only when the terminal model is valid.

The radical lifetime was measured at eight different values of f_1, including $f_1 = 1$ (we did not attempt to carry out the rotating-sector experiment at $f_1 = 0$ because pure MA gels too quickly to permit determination of the lifetime with any precision by this method). Typical examples of the $\bar{R}_p/R_{pL}$ vs. log t_L plot are presented in Figure 6, where $\bar{R}_p$ is the average rate of polymerization under intermittent illumination of light time t_L and dark time t_D ($t_D/t_L = 2$), and R_{pL} is the rate under steady illumination. Optimum values of lifetimes were determined by a least-squares

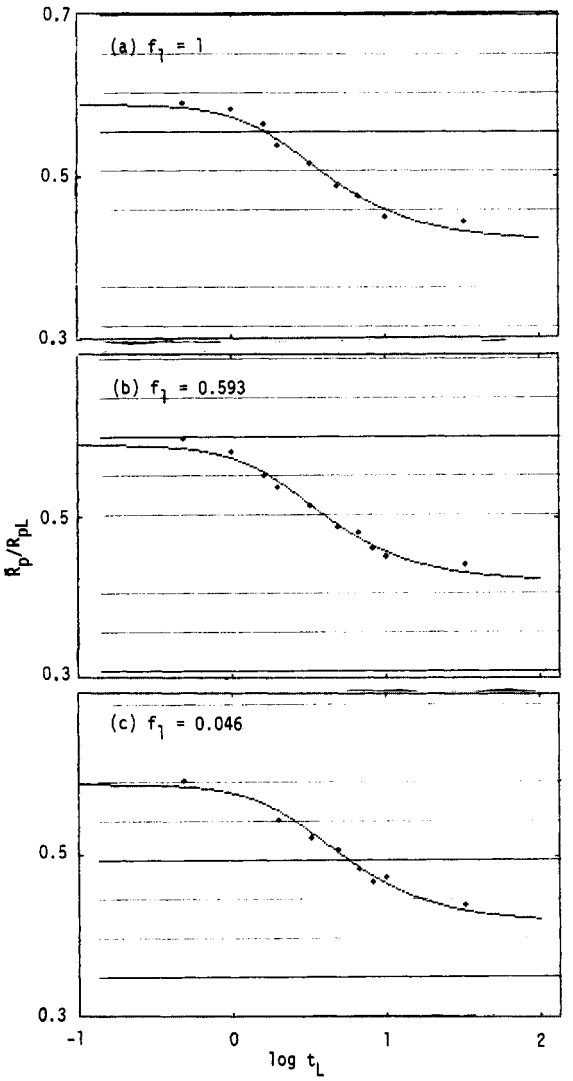

Figure 6. Plot of $\bar{R}_p/R_{pL}$ vs. log t_L for pCS/MA/ACN/40 °C systems for $t_D/t_L = 2$; (a) $f_1 = 1$, [ACN] = 8.41 × 10^{-3} mol L^{-1}, and $y = R_{pD}/R_{pL} = 0.130$; (b) $f_1 = 0.593$, [ACN] = 6.55 × 10^{-3}, and $y = 0.129$; (c) $f_1 = 0.046$, [ACN] = 8.51 × 10^{-3}, and $y = 0.125$.

curve-fitting method. The solid line in each figure represents the theoretical equation[1] calculated with the optimum value of lifetime. Numerical results are listed in Table III. These data were combined with the steady-run data to yield the individual values of k_p and k_t, which are listed in Table IV. These rate constant values are estimated to be correct to about 20% for k_p and about 40% for k_t in all cases.

We now compare these results with the predictions of some kinetic models. In Figure 7, the observed values of

Table IV
Values of the Rate Constants of Propagation and Termination for the Bulk Copolymerization of pCS and MA at 40 °C

f_1[a]	$10^2 k_p/k_t^{1/2}$,[b] $[(L/mol)/s]^{1/2}$	$10^5 k_p/k_t$[c]	k_p, (L/mol)/s	$10^{-6} k_t$, (L/mol)/s
0.046	3.00	0.613	147	24
0.114	2.01	0.391	103	26
0.233	1.81	0.339	97	29
0.360	1.78	0.415	76	18
0.443	1.80	0.382	85	22
0.593	1.86	0.312	111	36
0.757	1.88	0.333	106	32
1	1.95	0.304	125	41
		0.330	115	35

[a] Mole fraction of pCS in feed. [b] Value read from the solid curve in Figure 5. [c] From the rotating-sector experiments.

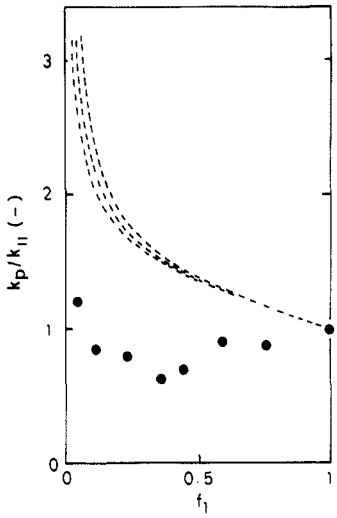

Figure 7. Plot of k_p/k_{11} vs. f_1 for the pCS/MA/40 °C system: the filled circles were measured, and the broken curves were calculated with the terminal model (eq 7 with $r_1 = 1.21$, $r_2 = 0.144$, $k_{11} = 120$ L mol^{-1} s^{-1}, and $k_{22} = 600$, 1200, and 3600 L mol^{-1} s^{-1}, from bottom upwards).

k_p are compared with those calculated with the terminal model

$$k_{p,term} = \frac{r_1 f_1^2 + 2f_1 f_2 + r_2 f_2^2}{(r_1 f_1/k_{11}) + (r_2 f_2/k_{22})} \tag{7}$$

where k_{ii} is identified with the k_p for the homopolymerization of monomer i. There are several literature values of k_{22} measured at various temperatures,[9] which suggest that k_{22} at 40 °C is of the order of 10^3 L mol^{-1} s^{-1}. The broken curves in Figure 7 were calculated by using our values of k_{11} and r_1 and r_2 and assuming three different values for k_{22} 600, 1200, and 3600 L mol^{-1} s^{-1}. Between the experimental data and any of the calculated curves are differences far exceeding the limit of experimental error. Curves calculated for $k_{22} > 3600$ almost coincide with the one for $k_{22} = 3600$, whereas it is unlikely that $k_{22} < 600$. Thus, even though a precise value of k_{22} is not available, we may unequivocally conclude that the propagation step of this system does not obey the terminal model.

This result was expected to some extent, since we already know the failure of the Mayo–Lewis equation to closely represent the composition of this system. As noted previously,[1] the propagation rate constant can generally be represented in the same form as eq 7

$$k_p = \frac{\bar{r}_1 f_1^2 + 2f_1 f_2 + \bar{r}_2 f_2^2}{(\bar{r}_1 f_1/\bar{k}_{11}) + (\bar{r}_2 f_2/\bar{k}_{22})} \tag{8}$$

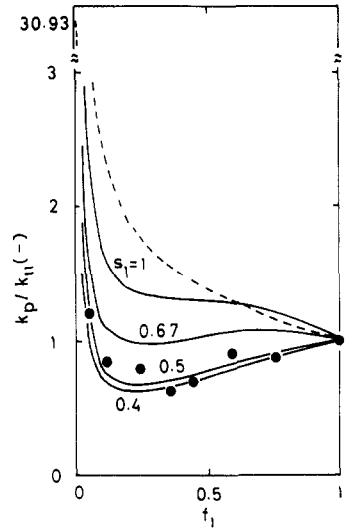

Figure 8. Plot of k_p/k_{11} vs. f_1 for the pCS/MA/40 °C system: the filled circles were measured, and the solid curves were calculated with the penultimate model (eq 8–11 with $r_1 = 0.92$, $r_1' = 2.3$, $r_2 = r_2' = 0.18$, $k_{111} = 120$ L mol^{-1} s^{-1}, $\bar{k}_{22} = 3600$ L mol^{-1} s^{-1} and s_1 as indicated in the figure). The broken curve represents the terminal model (cf. Figure 7).

where $\bar{r}_i$ and $\bar{k}_{ii}$ are, in general, functions of the composition of feed. Similarly, a generalized expression for the composition is the Mayo–Lewis equation with r_i's replaced by $\bar{r}_i$'s:

$$\frac{F_1}{F_2} = \frac{f_1(\bar{r}_1 f_1 + f_2)}{f_2(\bar{r}_2 f_2 + f_1)} \tag{9}$$

Clearly, the failure of the Mayo–Lewis equation is reflected on k_p through the composition dependence of $\bar{r}_i$'s. As already noted, the composition curve of this system is well represented by the penultimate model, for which $\bar{r}_1$, for example, is given by[1]

$$\bar{r}_1 = \frac{r_1'(f_1 r_1 + f_2)}{f_1 r_1' + f_2} \tag{10}$$

Assuming $\bar{k}_{ii}$'s to be constant ($\bar{k}_{11} = 120$ and $\bar{k}_{22} = 3600$ L mol^{-1} s^{-1}) and using the above-noted values of r_i and r_i', we calculated eq 8 with eq 10. The result is shown in Figure 8 by the solid curve indicated as $s_1 = 1$. As compared with the terminal model (the broken curve), the agreement with the experiment is somewhat improved, but by no means, sufficiently. This means that the main cause for the disagreement of the theory and experiment is the composition dependence of $\bar{k}_{ii}$ rather than $\bar{r}_i$. If we continue the analysis based on the penultimate model, for which $\bar{k}_{11}$, for example, is given by[1]

$$\bar{k}_{11} = \frac{k_{111}(r_1 f_1 + f_2)}{r_1 f_1 + (f_2/s_1)} \tag{11}$$

then we have the result given in Figure 8 (in the calculation, $\bar{k}_{22}$ was assumed to be constant, since the result is insensitive to $\bar{k}_{22}$ as already implied). The figure shows that the experimental data are well described by assuming s_1 ($=k_{211}/k_{111}$) to be about 0.5, indicating that the presence of a MA unit in the penultimate position significantly reduces the rate of pCS addition of the pCS radical. The implication obtained by this analysis should be ascertained by some other experimental and/or theoretical means. At present, our explanation, for the failure of the terminal model, in terms of penultimate effects is only tentative.[1]

Next we examine the termination step. In Figure 9, the observed values of k_t are plotted as a function of f_1. In-

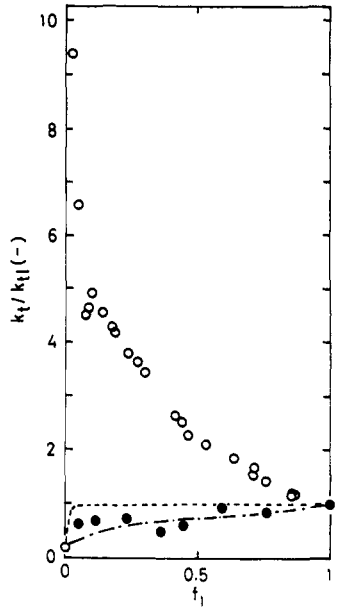

Figure 9. Plot of k_t/k_{t1} vs. f_1 for the pCS/MA/40 °C system: the filled circles were measured and the open circles were calculated from $k_t = (k_p/\omega)^2$ by using the experimental values of ω (Figure 5) and the terminal-model values of k_p (eq 7: the broken curve with k_{22} = 3600 L mol^{-1} s^{-1} in Figure 7). The broken curve represents the chemically controlled termination model with ϕ = 1, and the dot–dash curve represents the "ideal" diffusion model of North. $k_{t1} = 3.8 \times 10^7$ L mol^{-1} s^{-1}.

cluded in the figure are the values of k_t calculated from $k_t = (k_p/\omega)^2$ by using the experimental values of ω (Figure 5) and the terminal-model values of k_p (eq 7). Naturally, the calculated and observed results do not agree with each other, since the terminal model is not valid for this system. The large values of k_t obtained by the "calculation" correspond to the already-noted large values of ϕ. To be particularly noted is the magnitude of the observed values of k_t. As in the styrene/methyl methacrylate system studied previously,[1] the k_t values for the copolymerization are between those for the homopolymerizations at all compositions. This means that the termination step is well described by the chemically controlled termination model[4,10] with ϕ = 1 as well as by the "ideal" diffusion-controlled termination model[11] (see ref 1), as in fact Figure 9 shows (see the broken and dot–dash curves). In comparison of the two models, the diffusion model may appear to represent the experimental points slightly better than the ϕ = 1 model. In any case, it is implied, again,[1] that the termination reaction in copolymerization is described by a simple mechanism, much simpler than has hitherto been considered by many authors.[1]

Acknowledgment. We thank Tomofumi Yamamura for his contributions to this work at its early stage.

Registry No. pCS, 1073-67-2; MA, 96-33-3.

References and Notes

(1) Fukuda, T.; Ma, Y.-D.; Inagaki, H. *Macromolecules*, preceding paper in this issue.
(2) Dostal, H. *Monatsh. Chem.* **1936**, *69*, 424.
(3) (a) Mayo, F. R.; Lewis, F. M. *J. Am. Chem. Soc.* **1944**, *66*, 1954. (b) Alfrey, T., Jr.; Goldfinger, G. *J. Chem. Phys.* **1944**, *12*, 205. (c) Wall, F. T. *J. Am. Chem. Soc.* **1944**, *66*, 2050. (d) Sakurada, I. "Kojugo-Hanno"; Society of Polymer Chemistry, Japan: Tokyo, 1944.
(4) Walling, C. *J. Am. Chem. Soc.* **1949**, *71*, 1930.
(5) Fukuda, T.; Ma, Y.-D.; Inagaki, H. *Polym. J.* **1982**, *14*, 705.
(6) Ma, Y.-D.; Fukuda, T.; Yamamura, T.; Inagaki, H. *Polym. Prepr., Jpn.* **1981**, *30*, 56.
(7) Fukuda, T.; Ma, Y.-D.; Nagata, M.; Inagaki, H. *Polym. J.* **1982**, *14*, 729.
(8) Ma, Y.-D.; Fukuda, T.; Inagaki, H. *Polym. J.* **1983**, *15*, 673.
(9) Korus, R.; O'Driscoll, K. F. In "Polymer Handbook"; Brandrup, J., Immergut, E. H., Eds.; Academic Press: New York, 1975; Chapter II.
(10) Melville, H. W.; Noble, B.; Watson, W. F. *J. Polym. Sci.* **1947**, *2*, 229.
(11) Atherton, J. N.; North, A. M. *Trans. Faraday Soc.* **1962**, *58*, 2049.